Journal of Offshore Mechanics and Arctic Engineering. Received December 24, 2021; Accepted manuscript posted May 17, 2022. doi:10.1115/1.4054658

Journal of Offshore Mechanics and Arctic Engineering, Volume 144, Issue 4, August 2022, Paper number OMAE-21-1172

New tools to generate realistic ice floe fields for computational models

Luofeng Huang*
Lecturer in Mechanical Engineering
School of Water, Energy and Environment
Cranfield University
Cranfield, UK, MK43 0AL
Email: luofeng.huang@cranfield.ac.uk

Bojan Igrec
PhD Candidate in Naval Architecture
Department of Mechanical Engineering
University College London
London, UK, WC1E 6BT
Email: bojan.igrec.16@ucl.ac.uk

Giles Thomas
Professor in Maritime Engineering
Department of Mechanical Engineering
University College London
London, UK, WC1E 6BT
Email: giles.thomas@ucl.ac.uk

Global warming has extensively transformed Arctic sea ice from continuous level ice coverage to unconsolidated ice floe fields. Whilst the ice floes have a mixture of different sizes and their locations are randomly distributed, contemporary computational models lack effective methods to generate floe fields with such a natural pattern. This work introduces two original tools that can generate realistic ice floe fields for computational models. They are a sequential generator that sequentially handles ice floes one by one, and a genetic generator based upon a genetic algorithm. Demonstration of the tools is given, presenting samples of generating various shapes of floes and arbitrary mixtures of different shapes. Furthermore, an example is provided that combines the generated floe field with computational work modelling a ship transiting in ice floes. In addition, the source code of the tools is sharable to the public.

1 INTRODUCTION

Since the late 1970s when satellite observations began, the Arctic ice extent has decreased rapidly due to the effect of global warming [1]. The melting process has caused a widespread transformation of ice conditions in the Arctic, in particular, extensive unconsolidated ice floe fields have been replacing level-ice coverages, as shown in Fig. 1. With the transformation being ongoing, the ice floe environment has been reported to be a principal feature of the Arctic [2]. Also, the ice floe condition is dominant in the Antarctic [3, 4, 5].

The increasing ice floe fields play a significant role in both environmental and engineering areas. For example, it allows ocean surface waves to propagate through [6], which in turn dictates the ice extent, size and distribution. Contemporary climate models still cannot provide fully accurate predictions for Arctic ice evolution and global temperature change [7]. To improve this, a research gap is to appropriately integrate small-scale wave-ice interactions and floe-size distributions within large-scale climate models [8].

On the other hand, the ice floe environment is navigable for commercial ships without icebreaking capabilities, which led to the opening of numerous new shipping routes via the Arctic [9]. The new Arctic sea routes offer shorter voyage distances compared to their traditional counterparts and provide access to rich reserves of oil, gas, mines and fishing grounds. Yet, the ice floes that appear in the Arctic sea routes bring uncertainties to shipping operators, designers and builders, as there is the need to ascertain the additional resistance and structural loads from the floes on ships.

*Corresponding author.

Journal of Offshore Mechanics and Arctic Engineering. Received December 24, 2021;
Accepted manuscript posted May 17, 2022. doi:10.1115/1.4054658

Fig. 1: Ice floe fields emerging with climate change [4]

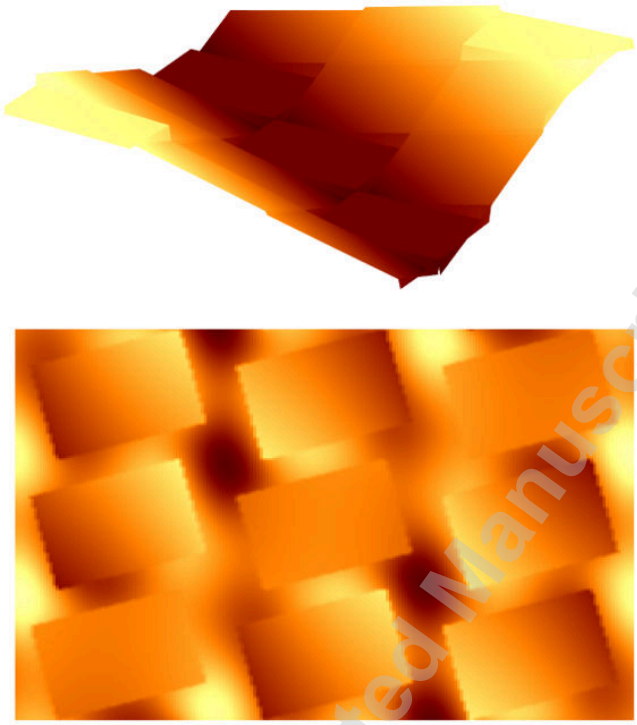

Fig. 2: The model of Porter [10] for simulating ocean waves propagating through an ice floe field, with regular floe size and distribution

2 PROBLEM DEFINITION

With the ongoing climate change, it is essential to build computational models for the environmental and engineering problems associated with the ice floe fields. However, there remain challenges to model ice-floe problems with high fidelity. For example, in computational models containing ice floe fields, the initial size and location of each floe need to be given, which is defined by the user based on assumptions. As a consequence, the modelled ice floe fields are usually imposed with subjective regularities. This may be seen in the model of Porter [10] studying the propagation of ocean waves through separated ice floes, the floes were set to be of uniform size and the distance between all the floes is initialised to be the same. It may be observed in Fig. 2 that the wave crests/troughs amongst the floes occur in regular locations, which is undesired due to its considerable influence on the propagation of wave energy. Thus, the model's prediction is dictated by the initial array that is subjectively defined.

The same issue can be seen in the model of Huang et al. [11] simulating a ship operating in ice floes, presented in Fig. 3. The ice loads on the ship are also dictated by the initial floe distribution, as the ship-ice contact points and angles are prescribed and a small change in the array can alter the ice impact. This kind of regular layout might provide acceptable accuracy for predicting average ice loads on structures, but would fail in predicting extreme loads or the distribution of loads on a hull.

This deficiency also appears in various existing models [12, 13, 14, 15, 16]. Moreover, multiple scholars have compared wave-ice and structure-ice interactions using different prescribed arrays of ice floes; they changed the row alignment and spacing, and proved that the influence of these subjectively-defined parameters on the prediction is essential [17, 18, 19, 20, 21]. These pieces of evidence indicate the need for methods that can replace the hypothetic regular floe fields with more natural floe fields, thus achieving high-fidelity reproduction of the reality.

Previous work on generating realistic ice floe fields for computational models has been given by [6, 22, 23, 24, 25, 26]. The work of Hopkins et al. [22] applied the approach of Voronoi tessellation and Delaunay triangulation, which was a theoretical approximation that did not match actual field measurements. The simulations of van den Berg et al. [23] and Yang et al. [24] used field and experimental images to reproduce the ice floes, but the image approach limits the size of the computational domain as well as the extension of the simulation for more scenarios. The methods of Montiel et al. [6], Metrikin [25] and Yulmetov et al. [26] have used field-measurement data of ice distribution law as input, while the floe shapes were limited to circular in [6] or random polygonal shapes in [25, 26].

To provide a more comprehensive approach for modelling ice floes, the present work introduces two different algorithms that can generate floe fields of any measured ice distribution law, and provide options to choose spe-

Journal of Offshore Mechanics and Arctic Engineering. Received December 24, 2021;
Accepted manuscript posted May 17, 2022. doi:10.1115/1.4054658

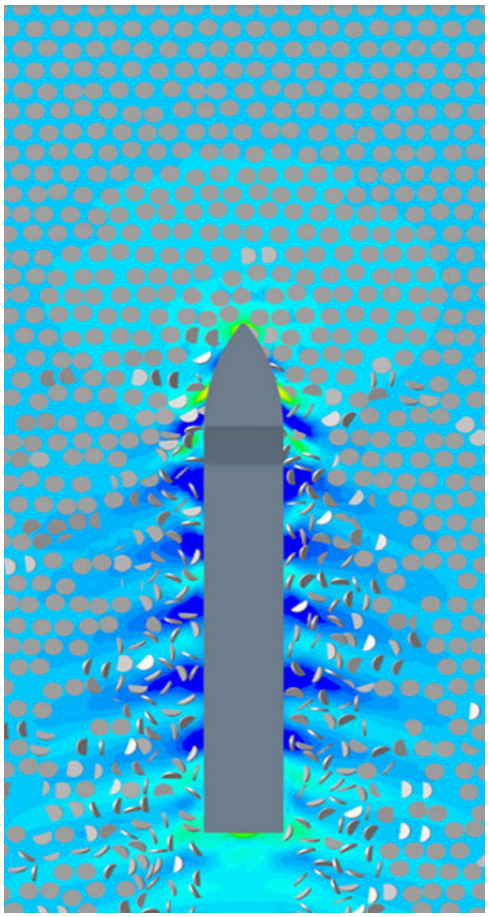

Fig. 3: The model of Huang et al. [11] for simulating a ship advancing in an ice floe field, with regular floe size and distribution

cific floe shapes (e.g. circular, triangular, square, rectangular and pentagonal) as well as arbitrary mixtures of different shapes in one domain.

Generating ice floe fields of arbitrary user-defined shapes can be beneficial for studying the underlying mechanism in different ice conditions, and for investigating the floe shape effect by comparing simulations of different shapes, as suggested by van den Berg et al. [23]. Also, the generated computational floe fields can match experiments that manufacture ice floes of designated shapes (usually using synthetic materials) [24]. In this way, the present work is expected to facilitate the development and validation of computational approaches for ice-floe problems. More importantly, the developed source code is intended to be shared with other researchers, which is the first open-source work providing such tools.

3 SOLUTIONS

In a natural ice floe field, the floes are of different sizes and their locations are randomly distributed. There are many types of sea ice floe varying in shape and size, two primary types are pancake ice and pack ice. In a sufficiently large region, the floe sizes of pancake and pack ice have been observed to distribute following a log-normal function [3, 27]; as shown in Fig. 4a, the majority of floes tend to have a size close to a medium value; the proportion for larger floes decreases with increased size, and the proportion for smaller floes decreases with decreased size. Such a curve is referred to as the curve of Floe-Size-Distribution (FSD). The FSD curve can have regional and seasonal variations, which can be obtained from field and aerial measurements [3, 28].

For both the generators in this work, an FSD curve is required as the governing input. Based on the FSD curve the total ice floes are divided into a certain number of groups, by different floe sizes; for each group, the floe size and the corresponding probability are extracted from the FSD curve, as shown in Fig. 4b. Fewer groups can be applied as long as the influence is negligible. For the size of a domain used to study an environmental or engineering problem in ice floe fields, the ice thickness of all floes usually does not have a notable variation [29], so the thickness of all floes in one computational domain is assumed to be constant; even so, the ice thickness can also be set to be varying if required. Other inputs include domain length and width of the specific computational model, the shape of the floes, and ice concentration (C, defined as the ice-covered area divided by the total sea-surface area, i.e. area of the domain). The complete condition of generating an ice floe field is that no overlapping occurs between any floes. Upon completion, the output is a matrix listing the $x - y$ coordinates of every ice floe and the corresponding floe size, while z coordinates are aligned to the buoyancy-gravity equilibration of each floe.

The first generator is a heuristic named Sequential Generator (SG), because it handles the floes one by one until all floes fulfil the complete condition. Based on the inputs, it first calculates the total number of ice floes (n_p), after which all floes are sorted by their decreasing sizes. Then, SG randomly positions ice floes into the computational domain, one by one, starting from the largest floe i = 1 to the smallest floe i = n_p. If overlapping occurs when SG is trying to position a floe, that floe will be randomly repositioned until it does not overlap with any previous floes; SG runs until all floes are successfully settled. During the process, SG changes only the position of the current ice floe while leaving all previously settled ice floes fixed. This can lead to a dead end, i.e. the fixed arrangement of previous ice floes may hinder subse-

Journal of Offshore Mechanics and Arctic Engineering. Received December 24, 2021;
Accepted manuscript posted May 17, 2022. doi:10.1115/1.4054658

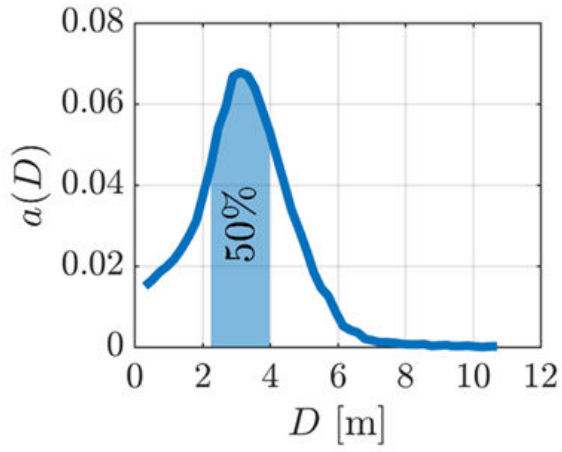

(a) Measured [3]

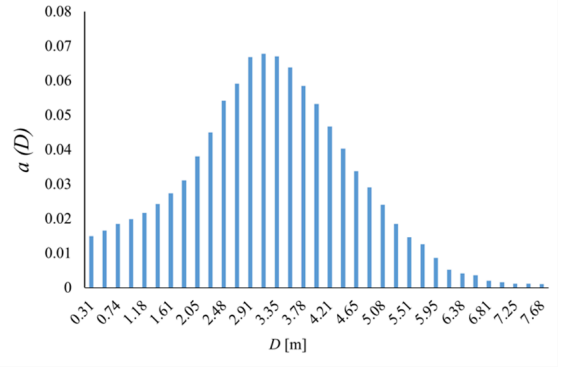

(b) Grouped

Fig. 4: An example of floe-size-distribution for pancake ice: the probability of occurrence (a) as a function of the floe diameter (D)

quent ice floes from being successfully settled. Therefore, a time-limit parameter is introduced to avoid this issue: if a solution has not been found within the time limit, the algorithm automatically restarts from the beginning. The time limit is suggested to be set at one minute for circular shape with any target C, while it may be increased for polygonal shapes with a high target C. Fig. 5 provides the flowchart of SG.

The second generator is named Genetic Generator (GG), because it is derived from the genetic algorithm based upon Darwin's principle: the survival of the fittest individuals [30]. GG defines a penalty factor to indicate the overlapping between ice floes; a higher penalty value corresponds to a higher overlapping area, i.e. an objective penalty factor of zero means no overlapping at all. GG starts by randomly producing a certain number (M_0) of initial solutions, corresponding to M_0 penalty values.

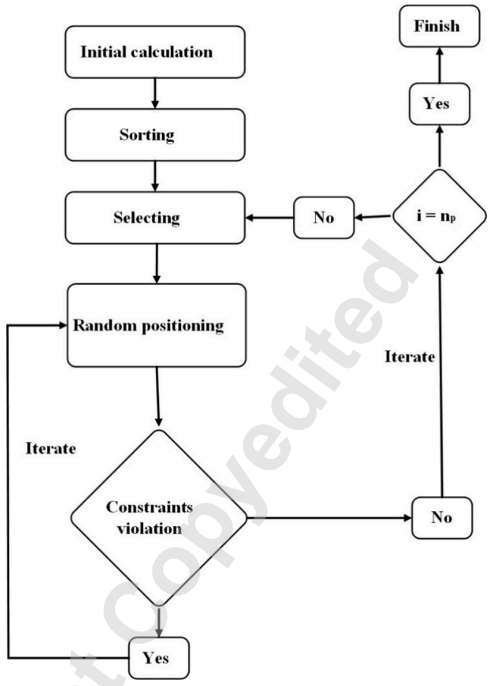

Fig. 5: Flowchart of SG

Subsequently, the algorithm selects a lower number of solutions (M_1) with averagely lower penalty values to be parents. By mixing parts of the parent solutions, M_0 child solutions are created, making up a total number of $M_0 + M_1$ solutions. Then M_0 solutions with the highest penalty values are discarded, and the total number of solutions goes back to M_0, but a better average penalty factor has been achieved. Additionally, M_2 solutions with best penalty factors are denoted as elite individuals, and in order to diversify non-elite solutions, random changes are applied to M_3 randomly chosen individuals from the group of non-elite solutions ($M_0 - M_2$). The above process is iterated from generation to generation until a solution is found that satisfies the objective penalty factor. Fig. 6 provides the flowchart of GG.

4 DEMONSTRATION

As reported by Toyota et al. [31], the shape of ice floes can vary with the common types including circular, triangular, rectangular, pentagonal, hexagonal (and arbitrary polygonal). There can also be multiple shapes of floes co-existing in a certain region. This work provides the capability to generate floes of a user-defined shape and as a mixture of multiple shapes. Meanwhile, aspect ratio is an important parameter for ice floes. For example, pancake ice floes are closer to ellipses than circles [3],

Journal of Offshore Mechanics and Arctic Engineering. Received December 24, 2021;
Accepted manuscript posted May 17, 2022. doi:10.1115/1.4054658

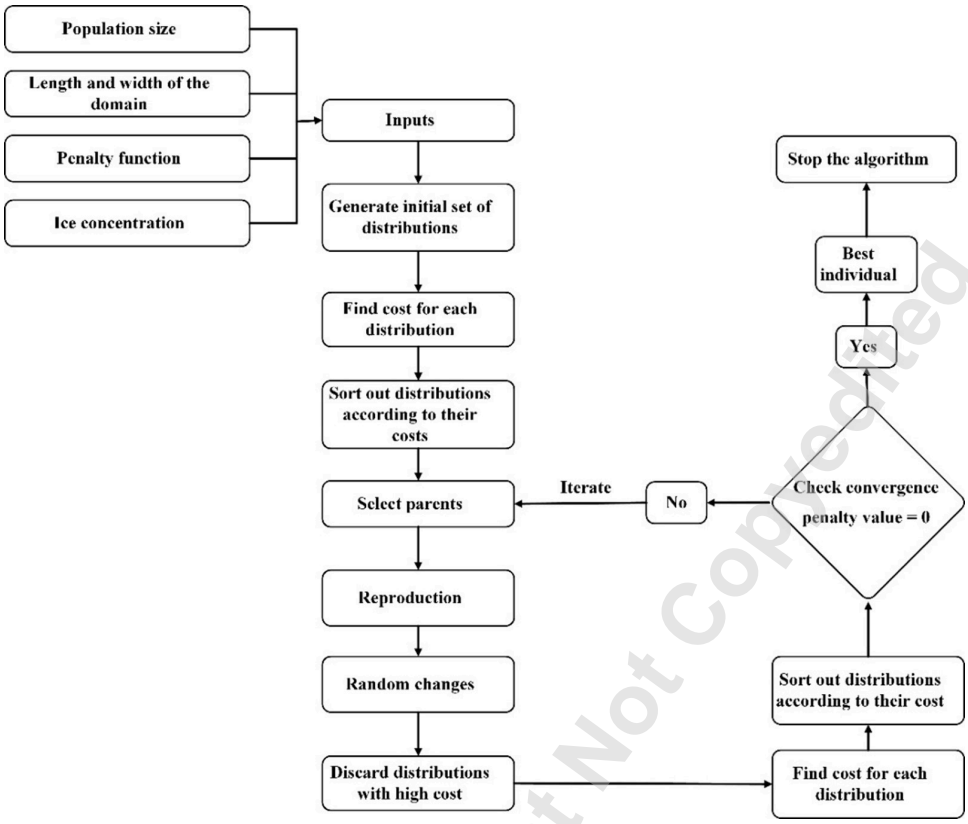

Fig. 6: Flowchart of GG

and ellipses are good approximations for wave-broken ice [32]. Hence, this work also offers the capability to define aspect ratio for floes. Examples of generated floe fields with different shapes and aspect ratios are given in Fig. 7.

Tests were run for both SG and GG for different ice concentration targets. It is seen that SG is a fast and oriented algorithm that the targeted FSD and C can be exactly achieved. The algorithm can generate an ice floe field within seconds, up to C = 70%, noting that the runtime scales with the total required computational domain (approximately linear with total floe number). However, SG gets slower when targetting $C > 70\%$; this is because a relatively high C means there is a limited open-water area in the domain, and thus it is hard for SG to settle all floes into desirable space. Therefore, SG is not recommended to be used for generating a solution of $C > 70\%$.

Unlike SG which considers only one solution at a time, GG handles a number of solutions simultaneously and requires multiple iterations. Thus the computational demand of GG is considerably higher than SG, where the runtime increases to an order of minutes. The intent for designing such an algorithm was to tackle very high ice concentrations for which SG would be unable to yield any solution in a reasonable time. Objective C = 75% and 80% have been attempted to be achieved using GG, as shown in Fig. 8, but a residual of 0.05-0.1% overlapping area could not be eliminated. The residual is not completely eliminable even after hours of iterating, which is reasonable as GG's algorithm is to select the optimal solutions while does not contain a step to enhance an optimal solution into a perfect solution. To further eliminate the residual, GG and partial SG may be coupled: GG could be performed to yield a solution with a minimal residual, followed by the "reposition" step of SG to find space to move the overlapping floes. This step may not be necessary in most cases, as the residual magnitude is very small. C = 80% is the highest concentration tested using GG, which is approximately the highest possible concentration of such floe fields without overlapping, e.g. Hopkins and Tuhkuri's experiments [33] show that C = 79% is the highest possible concentration, so $C > 80\%$ is out of the test scope here.

To further verify the algorithms and demonstrate their applicability, the tools have been used to generate pancake ice floe fields to replace the unrealistic floe fields shown in Fig. 3. The tools are easily compatible with the

Journal of Offshore Mechanics and Arctic Engineering. Received December 24, 2021;
Accepted manuscript posted May 17, 2022. doi:10.1115/1.4054658

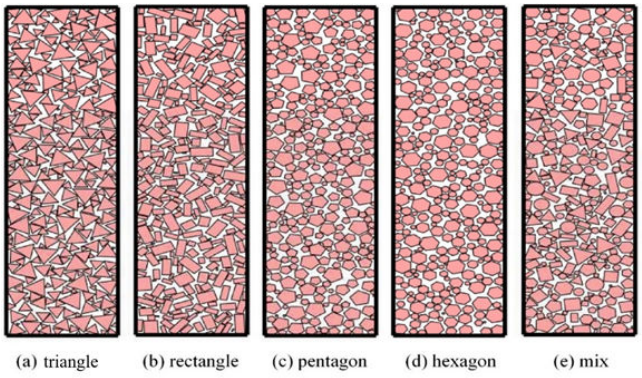

Fig. 7: Examples of generated ice floe fields with different shapes (C = 60%), in which, the rectangles' aspect ratio ranges from 1 to 3, and the mix contains six representative shapes (triangular, square, rectangular, pentagonal, hexagonal and circular)

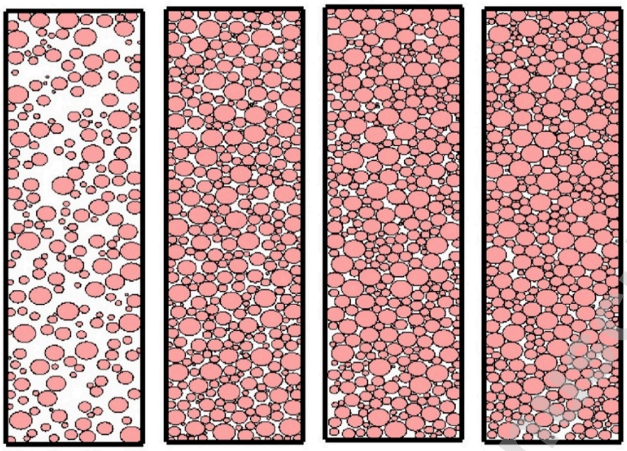

Fig. 8: Ice floe fields generated by SG, C = 40% and C = 70% (the left two); and by GG, C = 75% and C = 80% (the right two)

computational model, as the output is a list of floe dimensions and locations that can be directly used in the initial setups of a simulation. The updated ice floe fields are shown in Fig. 9, which was then used to investigate the resistance of ships advancing in emerging Arctic shipping routes infested by floating ice floes. Compared with using regular floe fields, the model's accuracy in predicting ice resistance has been evidently improved by the more realistic floe fields, with deviation level against experiments reduced from $< 30\%$ to $< 10\%$ [11, 34]. The work was further validated by full-scale measurements, which proved the floe fields generated using the present tools can be used to accurately predict ship fuel consumption and optimise shipping routes in the Arctic [35, 36, 37].

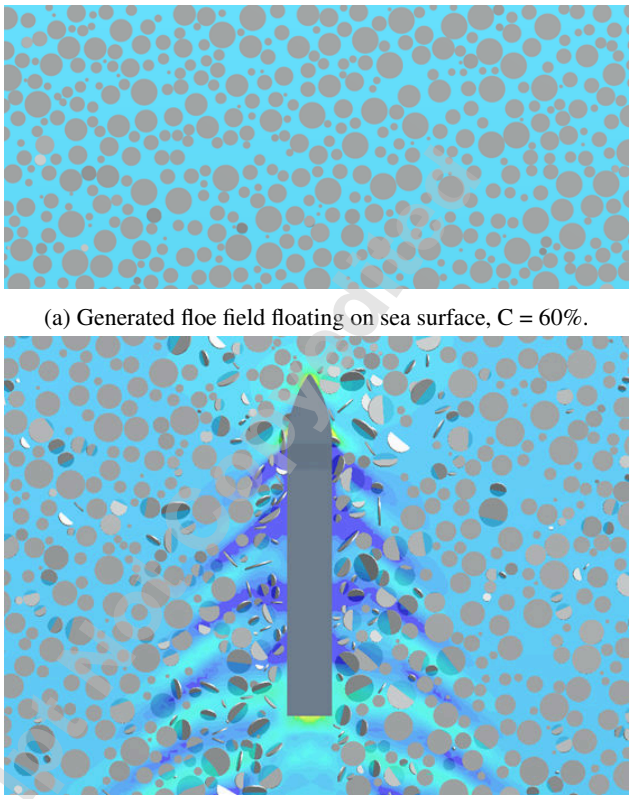

(a) Generated floe field floating on sea surface, C = 60%.

(b) A ship advancing in the generated floe field

Fig. 9: Demonstration of a computational model combined with a floe field generated by the code developed in this work

5 CONCLUSIONS

This work has provided and demonstrated two complementary algorithms that can effectively generate realistic ice floe fields for computational models. With climate change, the code facilitates the contemporary models with fidelity to represent increasing ice-floe conditions in polar regions, which is essential for investigating relevant environmental and engineering problems. An example of application has been presented with a computational model simulating the operation of a ship in floe-infested waterways. Other applications of this work could be studying structure-ice interactions [38, 39], the propagation of ocean waves in ice floe fields [40, 41], the collision and drift of floes [42, 43], as well as the associated thermodynamic and oceanographic modelling [7].

SOURCE CODE

The tools are written in MATLAB and instructions are given in the form of comments throughout the code. The authors intend to keep maintaining and developing the code. For requesting the latest version of the code or discussing additional functions, please email the corresponding author. The users are allowed to use/modify/develop the code for their own purposes, but the present paper should be cited where applicable.

REFERENCES

[1] Stroeve, J. C., Kattsov, V., Barrett, A., Serreze, M., Pavlova, T., Holland, M., and Meier, W. N., 2012, "Trends in arctic sea ice extent from cmip5, cmip3 and observations," *Geophysical Research Letters,* **39**(16).

[2] Thomson, J., Ackley, S., Girard-Ardhuin, F., Ardhuin, F., Babanin, A., Boutin, G., Brozena, J., Cheng, S., Collins, C., Doble, M., Fairall, C., Guest, P., Gebhardt, C., Gemmrich, J., Graber, H. C., Holt, B., Lehner, S., Lund, B., Meylan, M. H., Maksym, T., Montiel, F., Perrie, W., Persson, O., Rainville, L., Rogers, W. E., Shen, H., Shen, H., Squire, V., Stammerjohn, S., Stopa, J., Smith, M. M., Sutherland, P., and Wadhams, P., 2018, "Overview of the arctic sea state and boundary layer physics program," *Journal of Geophysical Research: Oceans*.

[3] Alberello, A., Onorato, M., Bennetts, L., Vichi, M., Eayrs, C., MacHutchon, K., and Toffoli, A., 2019, "Brief communication: Pancake ice floe size distribution during the winter expansion of the antarctic marginal ice zone," *The Cryosphere,* **13**(1), pp. 41–48.

[4] Alberello, A., Bennetts, L., Heil, P., Eayrs, C., Vichi, M., MacHutchon, K., Onorato, M., and Toffoli, A., 2020, "Drift of pancake ice floes in the winter antarctic marginal ice zone during polar cyclones," *Journal of Geophysical Research: Oceans,* **125**(3), p. e2019JC015418.

[5] Li, F., Lu, L., Suominen, M., and Kujala, P., 2021, "Short-term statistics of ice loads on ship bow frames in floe ice fields: Full-scale measurements in the antarctic ocean," *Marine Structures,* **80**, p. 103049.

[6] Montiel, F., Squire, V., and Bennetts, L., 2016, "Attenuation and directional spreading of ocean wave spectra in the marginal ice zone," *Journal of Fluid Mechanics,* **790**, pp. 492–522.

[7] Wadhams, P., 2017, *A farewell to ice: A report from the Arctic* Oxford University Press.

[8] Squire, V. A., 2020, "Ocean wave interactions with sea ice: a reappraisal," *Annual Review of Fluid Mechanics,* **52**, pp. 37–60.

[9] Smith, L. C., and Stephenson, S. R., 2013, "New trans-arctic shipping routes navigable by midcentury," *Proceedings of the National Academy of Sciences,* **110**(13), pp. E1191–E1195.

[10] Porter, R., 2019, "The coupling between ocean waves and rectangular ice sheets," *Journal of Fluids and Structures,* **84**, pp. 171–181.

[11] Huang, L., Li, M., Igrec, B., Cardiff, P., Stagonas, D., and Thomas, G., 2019, "Simulation of a ship advancing in floating ice floes," Port and Ocean Engineering under Arctic Conditions (POAC).

[12] Løset, S., 1994, "Discrete element modelling of a broken ice field—part ii: simulation of ice loads on a boom," *Cold regions science and technology,* **22**(4), pp. 349–360.

[13] Dai, M., Shen, H. H., Hopkins, M. A., and Ackley, S. F., 2004, "Wave rafting and the equilibrium pancake ice cover thickness," *Journal of Geophysical Research: Oceans,* **109**(C7).

[14] Sun, S., and Shen, H. H., 2012, "Simulation of pancake ice load on a circular cylinder in a wave and current field," *Cold Regions Science and Technology,* **78**, pp. 31–39.

[15] Janßen, C. F., Mierke, D., and Rung, T., 2017, "On the development of an efficient numerical ice tank for the simulation of fluid-ship-rigid-ice interactions on graphics processing units," *Computers & fluids,* **155**, pp. 22–32.

[16] Herman, A., Cheng, S., and Shen, H. H., 2019, "Wave energy attenuation in fields of colliding ice floes–part 1: Discrete-element modelling of dissipation due to ice–water drag," *The Cryosphere,* **13**(11), pp. 2887–2900.

[17] Peter, M. A., and Meylan, M. H., 2010, "Water-wave scattering by vast fields of bodies," *SIAM Journal on Applied Mathematics,* **70**(5), pp. 1567–1586.

[18] Williams, T. D., Bennetts, L. G., Squire, V. A., Dumont, D., and Bertino, L., 2013, "Wave–ice interactions in the marginal ice zone. part 1: Theoretical foundations," *Ocean Modelling,* **71**, pp. 81–91.

[19] Williams, T. D., Bennetts, L. G., Squire, V. A., Dumont, D., and Bertino, L., 2013, "Wave–ice interactions in the marginal ice zone. part 2: Numerical implementation and sensitivity studies along 1d transects of the ocean surface," *Ocean Modelling,* **71**, pp. 92–101.

[20] Bennetts, L., and Williams, T., 2015, "Water wave transmission by an array of floating discs," *Proceedings of the Royal Society A: Mathematical, Physical*

and Engineering Sciences, **471**(2173), p. 20140698.

[21] Guo, W., Zhao, Q.-s., Tian, Y.-k., and Zhang, W.-c., 2020, "Research on total resistance of ice-going ship for different floe ice distributions based on virtual mass method," *International Journal of Naval Architecture and Ocean Engineering,* **12**, pp. 957–966.

[22] Hopkins, M. A., Frankenstein, S., and Thorndike, A. S., 2004, "Formation of an aggregate scale in arctic sea ice," *Journal of Geophysical Research: Oceans,* **109**(C1).

[23] van den Berg, M., Lubbad, R., and Løset, S., 2019, "The effect of ice floe shape on the load experienced by vertical-sided structures interacting with a broken ice field," *Marine Structures,* **65**, pp. 229–248.

[24] Yang, B., Sun, Z., Zhang, G., Wang, Q., Zong, Z., and Li, Z., 2021, "Numerical estimation of ship resistance in broken ice and investigation on the effect of floe geometry," *Marine Structures,* **75**, p. 102867.

[25] Metrikin, I., 2014, "A software framework for simulating stationkeeping of a vessel in discontinuous ice,".

[26] Yulmetov, R., Lubbad, R., and Løset, S., 2016, "Planar multi-body model of iceberg free drift and towing in broken ice," *Cold Regions Science and Technology,* **121**, pp. 154–166.

[27] Colbourne, D., 2000, "Scaling pack ice and iceberg loads on moored ship shapes," *Oceanic Engineering International,* **4**(1), pp. 39–45.

[28] Parmiggiani, F., Moctezuma-Flores, M., Wadhams, P., and Aulicino, G., 2019, "Image processing for pancake ice detection and size distribution computation," *International Journal of Remote Sensing,* **40**(9), pp. 3368–3383.

[29] Roach, L. A., Smith, M. M., and Dean, S. M., 2018, "Quantifying growth of pancake sea ice floes using images from drifting buoys," *Journal of Geophysical Research: Oceans,* **123**(4), pp. 2851–2866.

[30] Holland, J. H., 1992, *Adaptation in natural and artificial systems: an introductory analysis with applications to biology, control, and artificial intelligence* MIT press.

[31] Toyota, T., Kohout, A., and Fraser, A. D., 2016, "Formation processes of sea ice floe size distribution in the interior pack and its relationship to the marginal ice zone off east antarctica," *Deep Sea Research Part II: Topical Studies in Oceanography,* **131**, pp. 28–40.

[32] Passerotti, G., Bennetts, L. G., Alberello, A., Puolakka, O., Dolatshah, A., Monbaliu, J., Toffoli, A., et al., 2021, "Interactions between irregular wave fields and sea ice: A physical model for wave attenuation and ice break up," *arXiv preprint arXiv:2110.12659*.

[33] Hopkins, M. A., and Tuhkuri, J., 1999, "Compression of floating ice fields," *Journal of Geophysical Research: Oceans,* **104**(C7), pp. 15815–15825.

[34] Huang, L., Tuhkuri, J., Igrec, B., Li, M., Stagonas, D., Toffoli, A., Cardiff, P., and Thomas, G., 2020, "Ship resistance when operating in floating ice floes: A combined cfd&dem approach," *Marine Structures,* **74**, p. 102817.

[35] Ryan, C., Huang, L., Li, Z., Ringsberg, J. W., and Thomas, G., 2021, "An arctic ship performance model for sea routes in ice-infested waters," *Applied Ocean Research,* **117**, p. 102950.

[36] Li, Z., Ryan, C., Huang, L., Ding, L., Ringsberg, J. W., and Thomas, G., 2021, "A comparison of two ship performance models against full-scale measurements on a cargo ship on the northern sea route," *Ships and Offshore Structures,* **16**(sup1), pp. 237–244.

[37] Huang, L., Li, Z., Ryan, C., Ringsberg, J. W., Pena, B., Li, M., Ding, L., and Thomas, G., 2021, "Ship resistance when operating in floating ice floes: Derivation, validation, and application of an empirical equation," *Marine Structures,* **79**, p. 103057.

[38] Hendrikse, H., and Nord, T. S., 2019, "Dynamic response of an offshore structure interacting with an ice floe failing in crushing," *Marine Structures,* **65**, pp. 271–290.

[39] Li, F., and Huang, L., 2022, "A review of computational simulation methods for a ship advancing in broken ice," *Journal of Marine Science and Engineering,* **10**(2), p. 165.

[40] Meylan, M., and Bennetts, L., 2018, "Three-dimensional time-domain scattering of waves in the marginal ice zone," *Philosophical Transactions of the Royal Society A: Mathematical, Physical and Engineering Sciences,* **376**(2129), p. 20170334.

[41] Huang, L., Ren, K., Li, M., Tuković, Ž., Cardiff, P., and Thomas, G., 2019, "Fluid-structure interaction of a large ice sheet in waves," *Ocean Engineering,* **182**, pp. 102–111.

[42] Yiew, L. J., Bennetts, L., Meylan, M., Thomas, G., and French, B., 2017, "Wave-induced collisions of thin floating disks," *Physics of Fluids,* **29**(12), p. 127102.

[43] Tavakoli, S., and Babanin, A. V., 2021, "Wave energy attenuation by drifting and non-drifting floating rigid plates," *Ocean Engineering,* **226**, p. 108717.